1 **GENERAL**

MAR-M-247 is the latest in the series of nickel-base alloys being offered for license under the patent rights of Martin-Marietta Corporation for use in applications requiring high strength capabilities at elevated temperatures. It is of the conventional gamma prime strengthened type with sufficient alloying present to generally form primary gamma prime in the as-cast condition. The composition contains only readily available elements balanced to provide maximum tensile, creep, and stress-rupture properties throughout the normal useful temperature range, i.e., up to about 2000 F, while maintaining freedom from secondary precipitation of all unwanted intermetallics, and of carbides of undesirable geometric shapes. Metallographic evaluation of creep specimens exposed up to 10,000 hr at all normal operating temperatures reveals excellent microstructural stability. This sluggish response to metallurgical rearrangement helps to provide and maintain excellent impact and notch toughness as well as high strength (6).

The composition of MAR-M-247 is also balanced to optimize castability. The alloy is readily castable into airfoil and integral wheel configurations by standard equiaxed precision lost-wax procedures and into directionally oriented and single crystal shapes by the withdrawal or exothermic processes (6).

The MAR-M-247 alloy is a version of MAR-M-246 which was initially modified only by the addition of hafnium; however, it was later found that the other elements also required modification in order to optimize properties and castability. The resulting alloy was redesignated as MAR-M-247 to distinguish it from the hafnium-modified version (MAR-M-246) in which the composition of the other elements had not yet been optimized.

1.01 **Commercial Designation**
MAR-M-247 (13).

1.02 **Alternate Designation**
MM-0011 (13).

1.03 **Specifications**
See Reference 2.

1.031 Aerospace Material Specification.

1.032 AiResearch specifications.

1.0321 Chemical composition shall be in accordance with AiResearch specification EMS 55447.

1.0322 All castings shall be visually, penetrant-, and X-ray-inspected in accordance with AiResearch specification EMS 52300.

1.0323 A master heat shall be made from AiResearch specification EMS 52330, Class I material.

1.0324 Each casting shall be identified with part number and master heat number in accordance with AiResearch specification MC5014.

1.0325 Castings shall be cleaned in accordance with AiResearch specification C5041.

1.05 **Heat Treatment**

1.051 Standard heat treatment for the alloy: 1600 F, 20 hr + AC.

1.052 Some studies require the alloy to be solution treated at 2250 F, 2 hr, argon quenched to below 1800 F, 5 hr + 1600 F, 20 hr + AC.

1.053 To evaluate the properties of coated specimens, uncoated specimens were used with heat treatment of 1800 F, 5 hr to simulate the coating cycle.

1.06 **Hardness**
Cast parts after heat treatment must have hardness of R_C 30 to 40 (2).

1.07 **Forms and Conditions Available**
Alloy available in investment castings and directionally solidified.

	Ni
10	Co
10	W
8.5	Cr
5.5	Al
0.7	Mo
3	Ta
1	Ti
1.4	Hf

MAR-M-247

1.08 **Melting and Casting Practice**

1.09 **Special Considerations**
Removal of cobalt from alloy improves the cyclic oxidation resistance and corrosion resistance.

1.091 Effect of reducing cobalt in nickel-base superalloy, Table 1.091.

2 **PHYSICAL AND CHEMICAL PROPERTIES**

2.01 **Thermal Properties**

2.011 Melting range: 2400 F to 2500 F.

2.012 Phase changes.

2.0121 Time-temperature-transformation diagrams.

2.013 Thermal conductivity of exothermally cast and directionally solidified alloy, Figure 2.013.

2.014 Thermal expansion of exothermally cast and directionally solidified alloy, Figure 2.014.

2.015 Specific heat.

2.016 Thermal diffusivity.

2.02 **Other Physical Properties**

2.03 **Chemical Properties**

2.031 No significant degradation was observed on RT-21 coated MAR-M-247 samples after 510 hr oxidation at 1900 F. However, the uncoated sample was heavily attacked by hot corrosion after 310 hr at 1700 F. (See Figure 2.034.) The alloy showed superior performance under hot corrosion relative to MAR-M-200 + Hf and NASA-TRN-R.

2.032 Cyclic oxidation behavior with and without protective aluminum-base RT-21 coating, Table 2.032.

2.033 Effect of cobalt content on oxidation resistance of the alloy, Figure 2.033.

2.034 Hot corrosion (in salt atmosphere) test results for exothermally cast and directionally solidified alloy, Figure 2.034.

2.04 **Nuclear Properties**

3 **MECHANICAL PROPERTIES**

3.01 **Specified Mechanical Properties**
Minimum room temperature properties specified by acceptance standard in Reference 2.

F_{tu} = 140 ksi
F_{ty} (0.2 percent) = 120 ksi
e (4D) = 7.0 percent
RA (4D) = 7.0 percent.

	Ni
10	Co
10	W
8.5	Cr
5.5	Al
0.7	Mo
3	Ta
1	Ti
1.4	Hf

MAR-M-247

3.02 **Mechanical Properties at Room Temperature**
See Section 3.03.

3.03 **Mechanical Properties at Various Temperatures**

3.031 Effect of temperature on tensile properties of equiaxed alloy, Figure 3.031.

3.0311 Tensile properties at room and elevated temperatures of longitudinal specimens machined from exothermally cast, directionally solidified turbine blades, Figure 3.0311.

3.0312 Tensile properties at room and elevated temperature of transverse specimens machined from exothermally cast, directionally solidified turbine blades, Figure 3.0312.

3.0313 Effect of directionally solidified grain orientation angle on the tensile ultimate and yield strength and the elastic modulus, Figure 3.0313.

3.0314 Effect of directionally solidified grain orientation angle on the tensile elongation and reduction of area, Figure 3.0314.

3.0315 Effect of cobalt level and temperature on yield strength, Figure 3.0315.

3.0316 Weibull plot showing comparison of tensile strengths of the alloy with IN-100 for specimens machined from integrally cast turbine wheel, Figure 3.0316.

3.0317 Weibull plot showing comparison of 0.2 percent yield strengths of the alloy with IN-100 for specimens machined from integrally cast turbine wheels, Figure 3.0317.

3.0318 Weibull plot showing comparison of elongations of the alloy with IN-100 for specimens machined from integrally cast turbine wheels, Figure 3.0318.

3.032 Compression.

3.034 Impact.

3.035 Torsion and shear.

3.036 Bearing.

3.037 Stress concentration.

3.0371 Notch properties, see also Sections 3.042, 3.053, 3.054, and 3.055.

3.0372 Fracture toughness.

3.038 Combined properties.

3.04 **Creep and Creep-Rupture Properties**

3.041 Stress for creep rupture in 100 and 1000 hr for bar machined from turbine blade, Figure 3.041.

3.042 Comparison of cyclic creep-rupture tests for smooth and notched specimens from exothermally DS cast slabs of MAR-M-247 with two other high strength nickel-base alloys, Figure 3.042.

3.043 Larson-Miller parameter plot for 0.5 percent creep strain of directionally solidified alloy, Figure 3.043.

3.044 Larson-Miller parameter plot for 1.0 percent creep strain of directionally solidified alloy, Figure 3.044.

3.045 Larson-Miller parameter plot for 2.0 percent creep strain of directionally solidified alloy, Figure 3.045.

3.046 Larson-Miller parameter plot for creep rupture of directionally solidified alloy, Figure 3.046.

3.047 Creep-rupture time and prior creep (elongation at 2 hr prior to rupture) of the alloy tested at 100.7 ksi and 1400 F, Figure 3.047.

3.048 Comparison of creep rupture time and elongation of two different heats of the alloy at 15.66 ksi and 1900 F, Figure 3.048.

3.049 Weibull probability plot of creep-rupture data from tests conducted at 40 ksi and 1650 F, Figure 3.049.

3.0410 Effect of crystallographic orientation on creep rupture life, Figure 3.0410.

3.0411 Effect of DS grain orientation on creep-rupture properties of the alloy and comparison with equiaxed alloy, Figure 3.0411.

3.0412 Larson-Miller plot showing the effect of cobalt level on creep-rupture strength, Figure 3.0412.

3.0413 Effect of cobalt level on the alloy on creep-rupture ductility, Figure 3.0413.

3.0414 Effect of cobalt content on creep rate, Figure 3.0414.

3.0415 Effect of cobalt content on time to onset of tertiary creep, Figure 3.0415.

3.0416 Effect of cobalt content on creep characteristics of the alloy at 1400 F, 100 ksi and 1600 F, 60 ksi, Figure 3.0416.

3.0417 Effect of cobalt content on creep rupture and steady state creep rate at 1600 F, Figure 3.0417.

3.0418 Effect of cobalt content on creep rupture and steady state creep rate at 1400 F, 100 ksi and 1800 F, 25 ksi, Figure 3.0418.

3.0419 Effect of zirconium contamination on creep-rupture lives of specimens machined from single crystal blades in longitudinal direction, Figure 3.0419.

3.0420 Larson-Miller parameters for creep rupture of directionally solidified and equiaxed alloy, Figure 3.0420.

3.0421 Larson-Miller parameters for creep rupture of directionally solidified MAR-M-247 and equiaxed IN-100, Figure 3.0421.

3.0422 Comparison of Larson-Miller parameters for creep rupture of equiaxed MAR-M-247 and IN-100, Figure 3.0422.

3.05 **Fatigue Properties**

3.051 Low cycle fatigue tests under load control at 1400 F for smooth uncoated specimens from separately cast test bars, Figure 3.051.

3.052 Low cycle fatigue tests under load control at 1400 F for smooth coated specimens from separately cast test bars, Figure 3.052.

3.053 Low cycle fatigue tests under load control at 1400 F for notched uncoated specimens from separately cast test bars, Figure 3.053.

3.054 Load controlled high cycle fatigue tests for smooth and notched specimens at room temperature, Figure 3.054.

3.055 Load controlled high cycle fatigue tests for smooth and notched specimens at 1600 F, Figure 3.055.

3.056 Estimated endurance limits at 10^7 cycles from load controlled axial high cycle fatigue tests, Figure 3.056.

3.057 Effect of grain orientation on thermal fatigue life of the alloy in the coated and uncoated condition, Figure 3.057.

3.06 **Elastic Properties**

3.061 Poisson's ratio.

3.062 Modulus of elasticity.

3.0621 Modulus of elasticity in longitudinal grain orientation for test specimens machined from exothermally cast directionally-solidified alloy, Figure 3.0621.

3.063 Modulus of rigidity.
3.064 Tangent modulus.
3.065 Secant modulus.

4 FABRICATION

4.01 Forming

4.02 Machining and Grinding

4.03 Joining

4.04 Surface Treating

REFERENCES

1 The International Nickel Company, Inc., "High Temperature, High Strength Nickel Base Alloys" (July 1977).

2 Sink, L. W., Hoppin, G. S. III, and Fujii, M., "Low Cost Directionally-Solidified Turbine Blades", NASA CR-159464, AiResearch 21-2953 (January 1979) p 243-247.

3 Bizon, P. T., Dreshfield, R. L., and Calfo, F. D., "Effect of Grain Orientation and Casting on Thermal Fatigue Resistance of a Directionally-Solidified Superalloy MAR-M-247", NASA TM-79129 (April 1979).

4 MacKay, A. R., Dreshfield, R. L., and Maier, R. D., "Anisotropy of Nickel-Base Superalloy Single Crystals", Metallurgical Transactions, Vol 13A (October 1982).

5 Harris, K., Schwer, R. E., "Vacuum Induction Refined MM0011 (MAR-M-247) For Investment Cast Turbine Components", Sixth International Vacuum Metallurgy Conference, International Conference on Special Melting, San Diego, California, Cannon-Muskegan Corp, Muskegan, Michigan (April 23-27, 1979).

6 Martin-Marietta Corporation. Special communication to MCIC (1979).

7 NASA Third Annual 'MATE' Review (March 29, 1979).

8 Harris, K., and Schwer, R. E., "Vacuum Induction Refining MM0011 (MAR-M-247) For High Integrity Turbine Rotating Parts", TMS-AIME Fall Meeting in St. Louis (October 1978).

9 Nathal, M. V., Maier, R. D., and Ebert, L. J., "The Influence of Cobalt on the Tensile and Stress-Rupture Properties of the Nickel-Base Superalloy MAR-M-247", Metallurgical Transactions, Vol 13A (1982) p 1767-1774.

10 Stephens, J. R., "A Status Review of NASA's COSAM (Conservation of Strategic Aerospace Materials) Program", NASA TM-82852 (May 1982).

11 Stoloff, N. S., in Alloy and Microstructural Design, edited by J. K. Tien and G. S. Ansell, Academic Press, New York (1976) p 104.

12 Kear, B. H., and Piearcey, B. J., Transactions TMS-AIME, Vol. 239 (1967) p 1209-1215.

13 Martin-Marietta Corporation, Patents 3,677,747 and 3,720,509.

	Ni
10	Co
10	W
8.5	Cr
5.5	Al
0.7	Mo
3	Ta
1	Ti
1.4	Hf

MAR-M-247

Alloy	MAR-M-247		
	Weight Percent		
Composition	Min	Max	Suggested Aim
Co	9.0	11.0	10.0
W	9.5	10.5	10.0
Cr	8.0	8.8	8.25
Al	5.3	5.7	5.5
Ta	2.8	3.3	3.0
Hf	1.2	1.6	1.5
Ti	0.9	1.2	1.0
Mo	0.5	0.8	0.7
C	0.13	0.17	0.15
Zr	0.03	0.08	0.05
B	0.01	0.02	0.015
Mg	–	0.20	–
S	–	0.015	–
Si	–	0.20	–
Fe	–	0.50	–
Ni	Remainder		

TABLE 1.041. COMPOSITION (2)

Property	Reducing Cobalt
Tensile Properties	Minimal Effect
Rupture Life	50 percent Reduction – Slight Decrease Total Removal – Major Decrease
Creep Rate	50 percent Reduction – Slight Increase Total Removal – Major Increase
Oxidation Resistance	Improves
Corrosion Resistance	Improves
Long Term Stability	Improves

Contributing Factors

γ' Volume Fraction
Carbide Morphology and Composition
Stacking Fault Energy
γ - γ' Mismatch

TABLE 1.091. EFFECT OF REDUCING COBALT IN NICKEL-BASE SUPERALLOYS (10)

	Ni
10	Co
10	W
8.5	Cr
5.5	Al
0.7	Mo
3	Ta
1	Ti
1.4	Hf

MAR-M-247

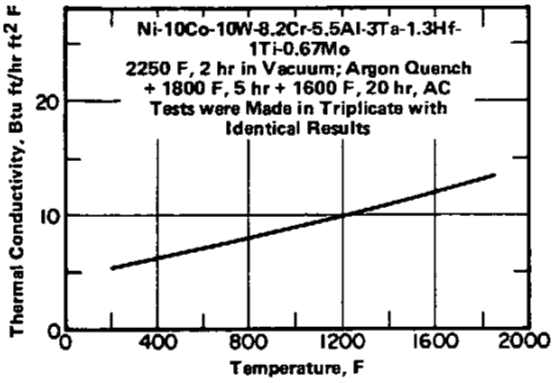

FIGURE 2.013. THERMAL CONDUCTIVITY OF EXOTHERMALLY CAST AND DIRECTIONALLY SOLIDIFIED ALLOY (2)

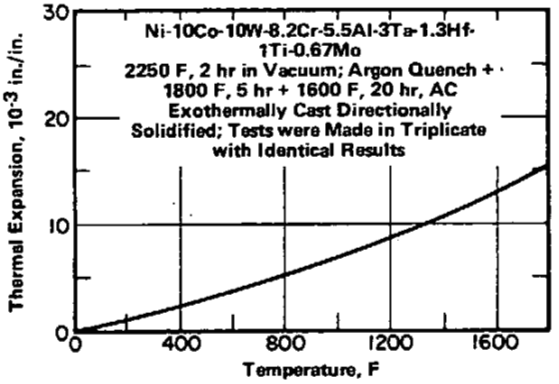

FIGURE 2.014. THERMAL EXPANSION OF EXOTHERMALLY CAST AND DIRECTIONALLY SOLIDIFIED ALLOY (2)

Ni-10Co-10W-8.2Cr-5.5Al-3Ta-1.3Hf-1Ti-0.67Mo
2250 F, 2 hr in Vacuum; Argon Quench + 1800 F, 5 hr + 1600 F, 20 hr, AC
Exothermally Cast, Directionally Solidified
Jet A Fuel, 60 min, Hot (1900 F); 3 min, Cold
1500 rpm Specimen Rotation in AiResearch Oxidation,
Hot-Corrosion, Test Rig (See Figure 2.034)
Weight Change is an Average of Two Test Specimens

	Weight Change in Grams at Indicated Test Time in Hours								
Alloy	25	60	80	110	210	300	400	510	Remark
RT-21 Coated	+0.01	+0.01	+0.01	+0.01	-0.01	-0.01	-0.01	-0.01	No Coating Degradation
Uncoated	0	0	0	0	-0.02	-0.01	-0.01	-0.01	Slight Oxidation

TABLE 2.032. CYCLIC OXIDATION BEHAVIOR WITH AND WITHOUT PROTECTIVE ALUMINUM-BASE RT-21 COATING (2)

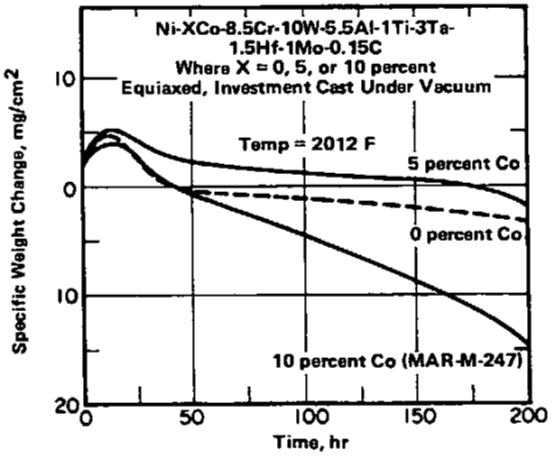

FIGURE 2.033. EFFECT OF COBALT CONTENT ON OXIDATION RESISTANCE OF THE ALLOY (10)

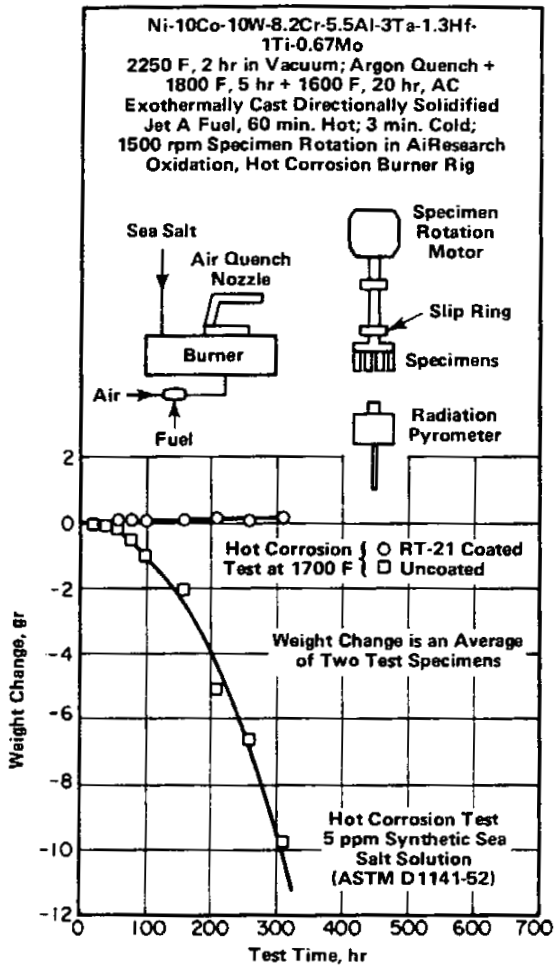

FIGURE 2.034. HOT CORROSION (IN SALT ATMOSPHERE) TEST RESULTS FOR EXOTHERMALLY CAST, AND DIRECTIONALLY SOLIDIFIED ALLOY (2)

	Ni
10	Co
10	W
8.5	Cr
5.5	Al
0.7	Mo
3	Ta
1	Ti
1.4	Hf

MAR-M-247

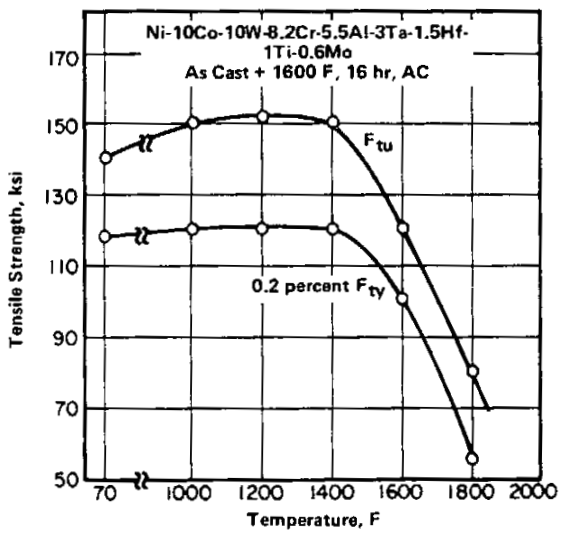

FIGURE 3.031. EFFECT OF TEMPERATURE ON TENSILE PROPERTIES OF EQUIAXED ALLOY (1)

	Ni
10	Co
10	W
8.5	Cr
5.5	Al
0.7	Mo
3	Ta
1	Ti
1.4	Hf

MAR-M-247

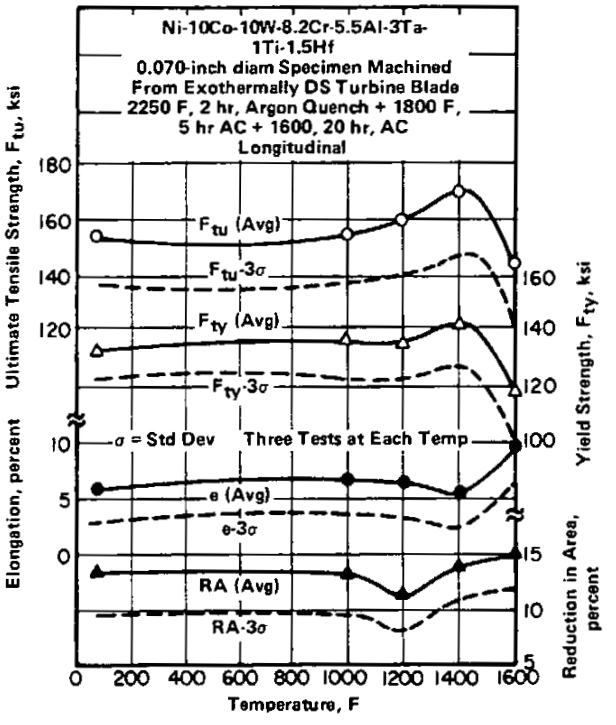

FIGURE 3.0311. TENSILE PROPERTIES AT ROOM AND ELEVATED TEMPERATURES OF LONGITUDINAL SPECIMENS MACHINED FROM EXOTHERMALLY CAST, DIRECTIONALLY SOLIDIFIED TURBINE BLADES (2)

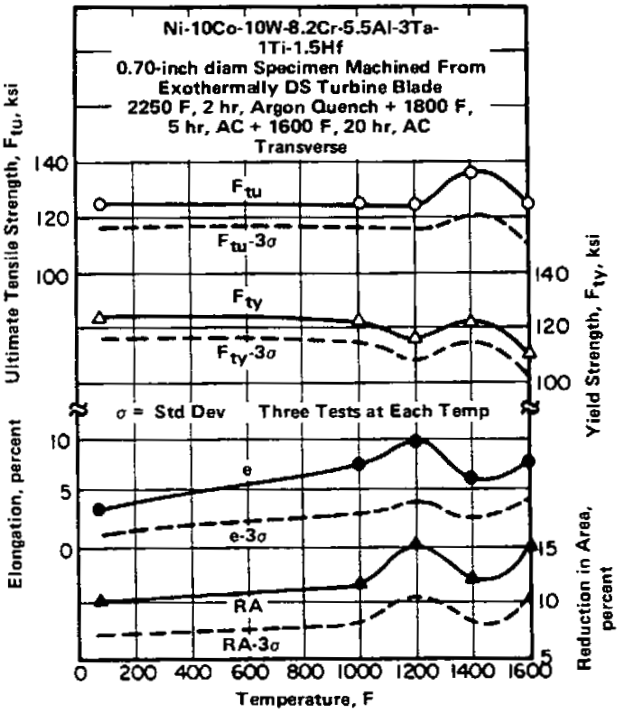

FIGURE 3.0312. TENSILE PROPERTIES AT ROOM AND ELEVATED TEMPERATURE OF TRANSVERSE SPECIMENS MACHINED FROM EXOTHERMALLY CAST, DIRECTIONALLY SOLIDIFIED TURBINE BLADES (2)

	Ni
10	Co
10	W
8.5	Cr
5.5	Al
0.7	Mo
3	Ta
1	Ti
1.4	Hf

MAR-M-247

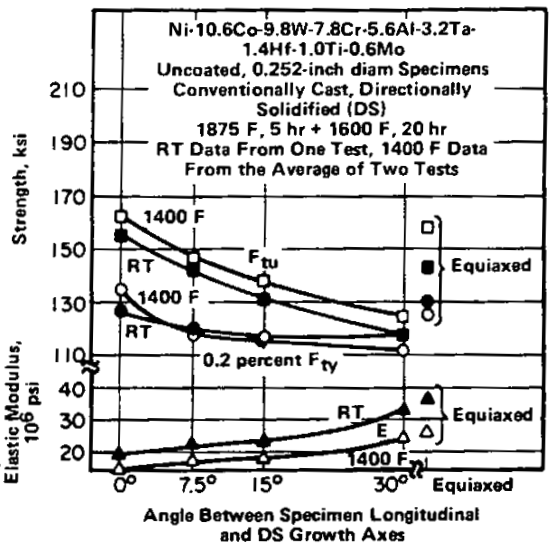

FIGURE 3.0313. EFFECT OF DIRECTIONALLY SOLIDIFIED GRAIN ORIENTATION ANGLE ON THE TENSILE ULTIMATE AND YIELD STRENGTH AND THE ELASTIC MODULUS (3)

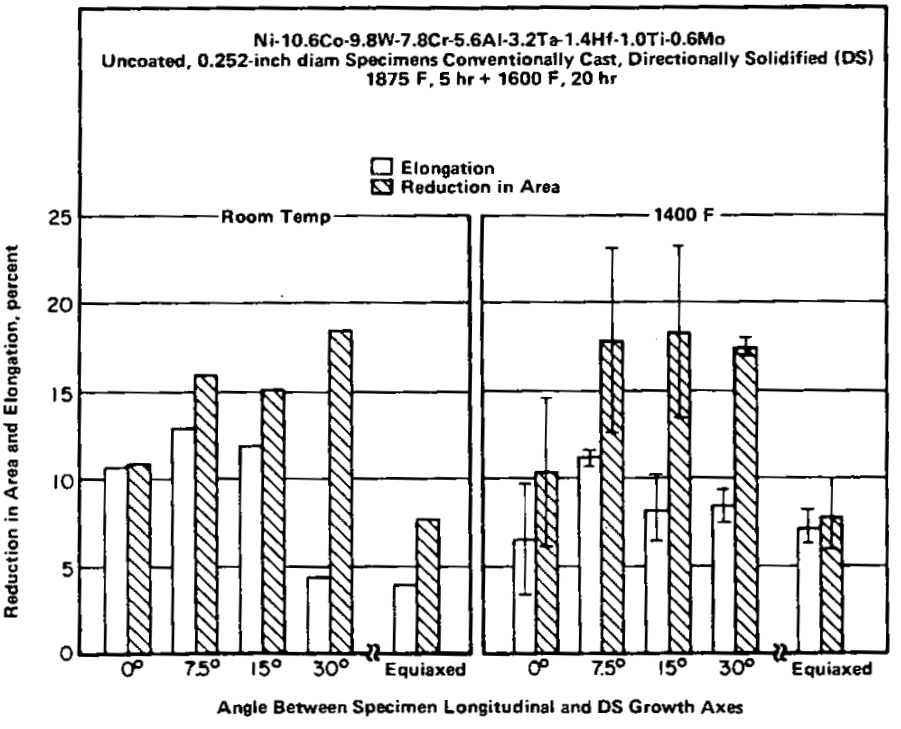

FIGURE 3.0314. EFFECT OF DIRECTIONALLY SOLIDIFIED GRAIN ORIENTATION ANGLE ON THE TENSILE ELONGATION AND REDUCTION OF AREA (3)

	Ni
10	Co
10	W
8.5	Cr
5.5	Al
0.7	Mo
3	Ta
1	Ti
1.4	Hf

MAR-M-247

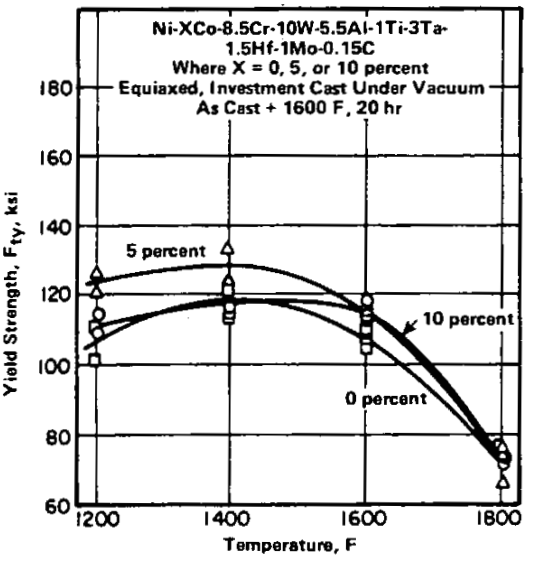

FIGURE 3.0315. EFFECT OF COBALT LEVEL AND TEMPERATURE ON YIELD STRENGTH (9)

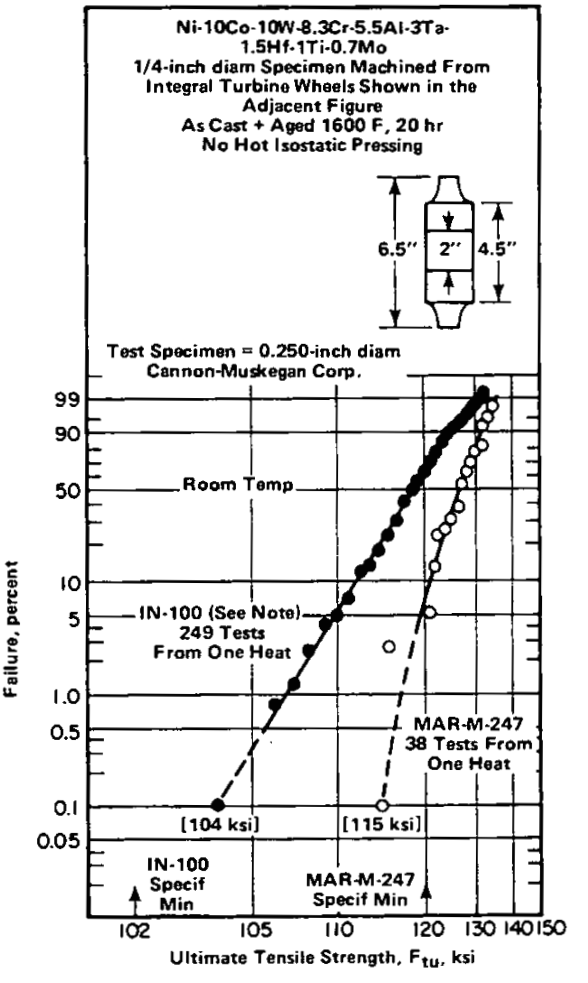

FIGURE 3.0316. WEIBULL PLOT SHOWING COMPARISON OF TENSILE STRENGTHS OF THE ALLOY WITH IN-100 FOR SPECIMENS MACHINED FROM INTEGRALLY CAST TURBINE WHEEL (5)

Note: IN-100 is a Ni-base alloy with 1.5Co-10Cr-5.5Al-4.7Ti-3Mo-0.95V.

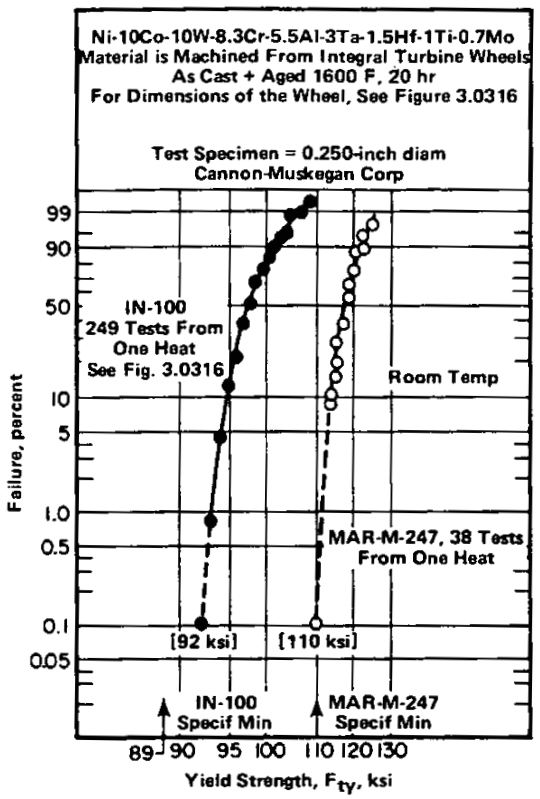

FIGURE 3.0317. WEIBULL PLOT SHOWING COMPARISON OF 0.2 PERCENT YIELD STRENGTHS OF THE ALLOY WITH IN-100 FOR SPECIMENS MACHINED FROM INTEGRALLY CAST TURBINE WHEELS (5)

	Ni
10	Co
10	W
8.5	Cr
5.5	Al
0.7	Mo
3	Ta
1	Ti
1.4	Hf

MAR-M-247

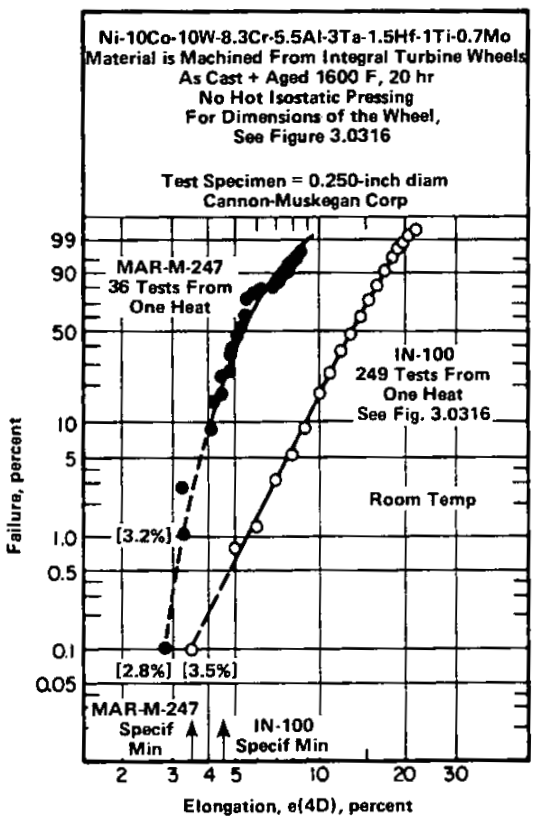

FIGURE 3.0318. WEIBULL PLOT SHOWING COMPARISON OF ELONGATIONS OF THE ALLOY WITH IN-100 FOR SPECIMENS MACHINED FROM INTEGRALLY CAST TURBINE WHEELS (5)

	Ni
10	Co
10	W
8.5	Cr
5.5	Al
0.7	Mo
3	Ta
1	Ti
1.4	Hf

MAR-M-247

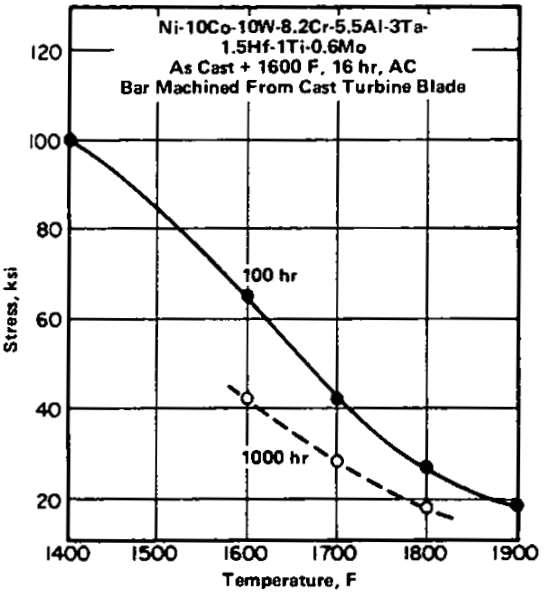

FIGURE 3.041. STRESS FOR CREEP RUPTURE IN 100 AND 1000 HR FOR BAR MACHINED FROM TURBINE BLADE (1)

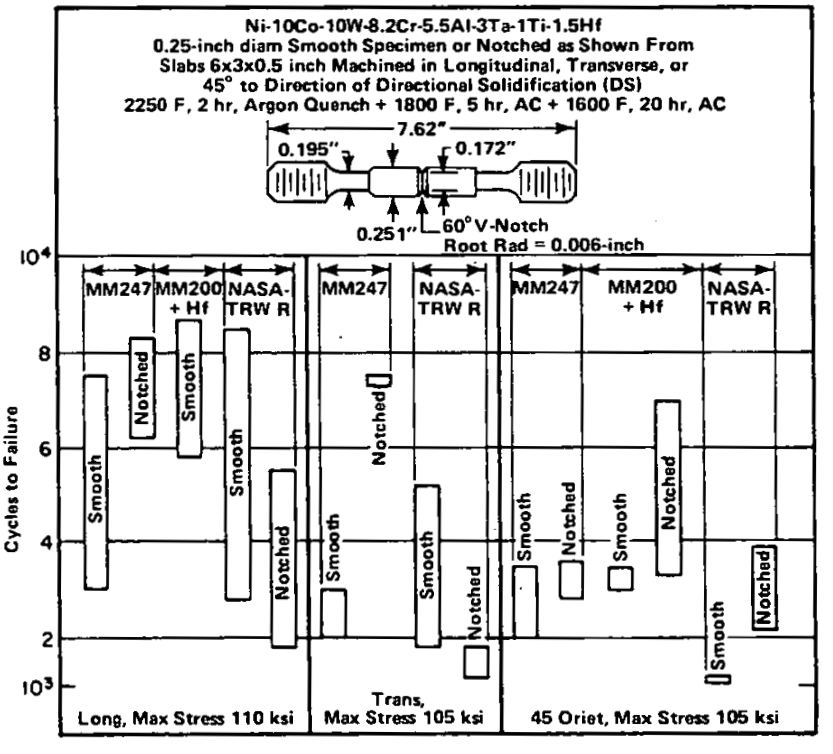

FIGURE 3.042. COMPARISON OF CYCLIC CREEP-RUPTURE TESTS FOR SMOOTH AND NOTCHED SPECIMENS FROM EXOTHERMALLY DS CAST SLABS OF MAR-M-247 WITH TWO OTHER HIGH STRENGTH NICKEL-BASE ALLOYS (2)

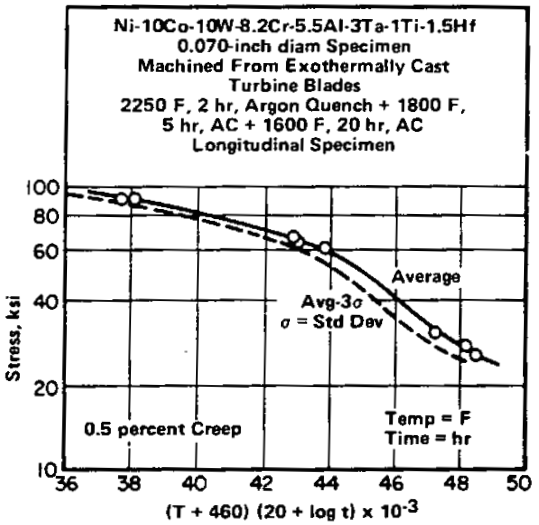

FIGURE 3.043. LARSON-MILLER PARAMETER PLOT FOR 0.5 PERCENT CREEP STRAIN OF DIRECTIONALLY SOLIDIFIED ALLOY (2)

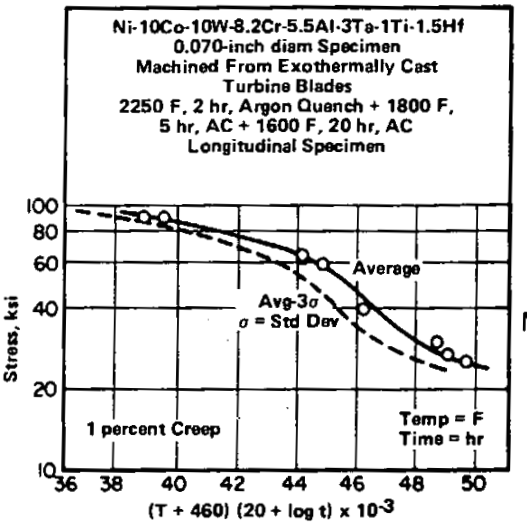

FIGURE 3.044. LARSON-MILLER PARAMETER PLOT FOR 1.0 PERCENT CREEP STRAIN OF DIRECTIONALLY SOLIDIFIED ALLOY (2)

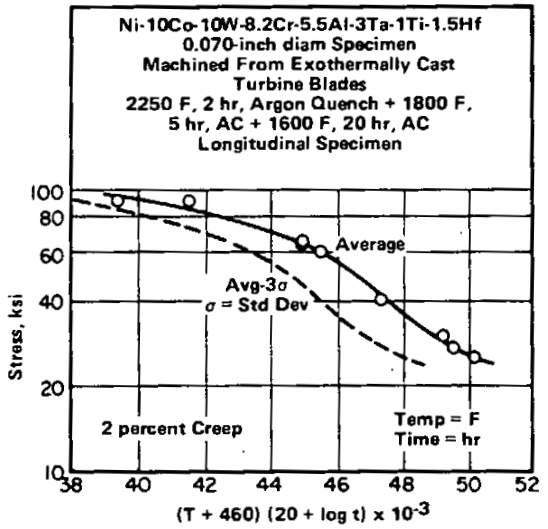

FIGURE 3.045. LARSON-MILLER PARAMETER PLOT FOR 2.0 PERCENT CREEP STRAIN OF DIRECTIONALLY SOLIDIFIED ALLOY (2)

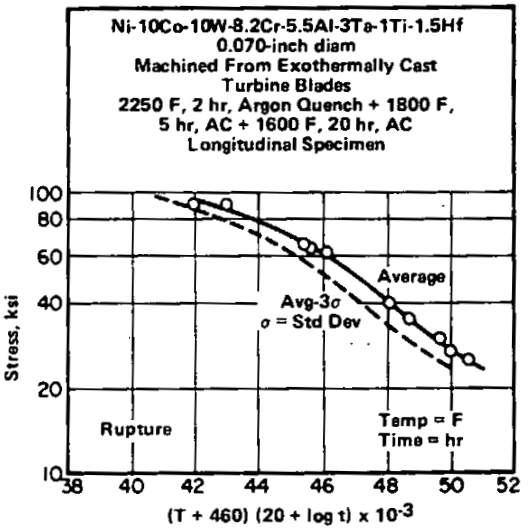

FIGURE 3.046. LARSON-MILLER PARAMETER PLOT FOR CREEP RUPTURE OF DIRECTIONALLY SOLIDIFIED ALLOY (2)

	Ni
10	Co
10	W
8.5	Cr
5.5	Al
0.7	Mo
3	Ta
1	Ti
1.4	Hf

MAR-M-247

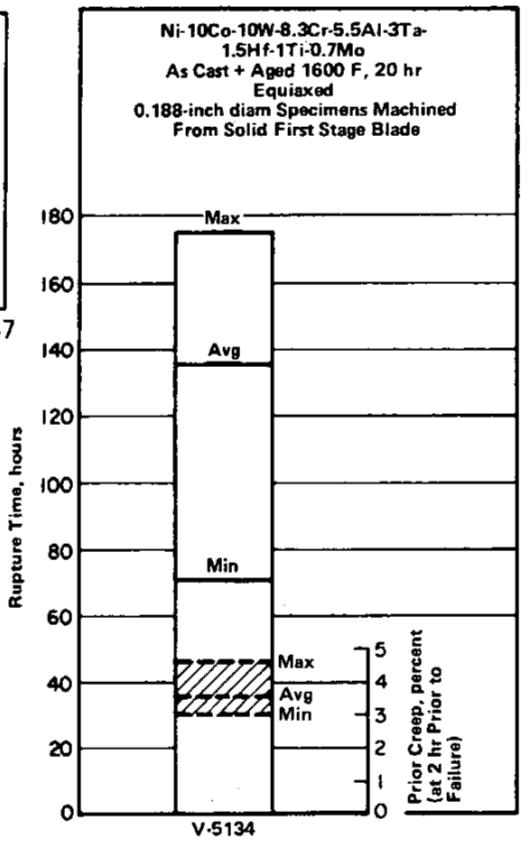

FIGURE 3.047. CREEP-RUPTURE TIME AND PRIOR CREEP (ELONGATION AT 2 HR PRIOR TO RUPTURE) OF THE ALLOY TESTED AT 100.7 KSI AND 1400 F (8)

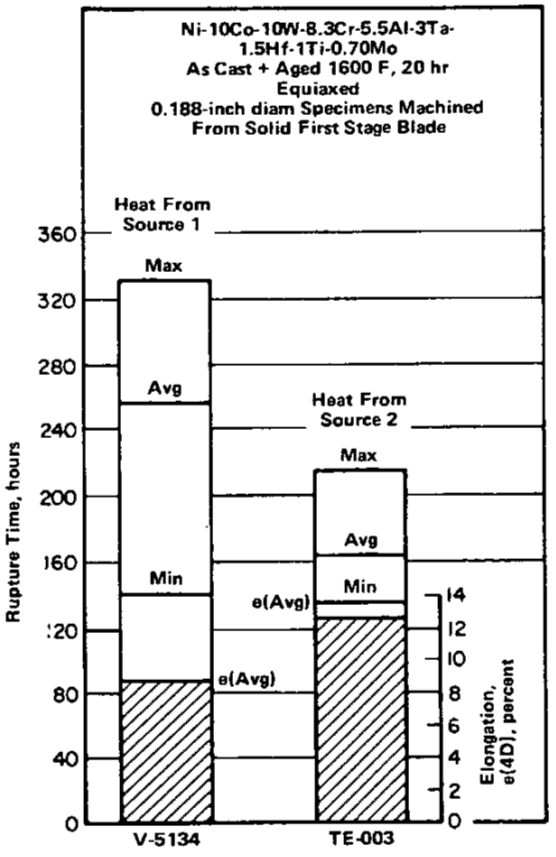

FIGURE 3.048. COMPARISON OF CREEP RUPTURE TIME AND ELONGATION OF TWO DIFFERENT HEATS OF THE ALLOY AT 15.66 KSI AND 1900 F (8)

	Ni
10	Co
10	W
8.5	Cr
5.5	Al
0.7	Mo
3	Ta
1	Ti
1.4	Hf

MAR-M-247

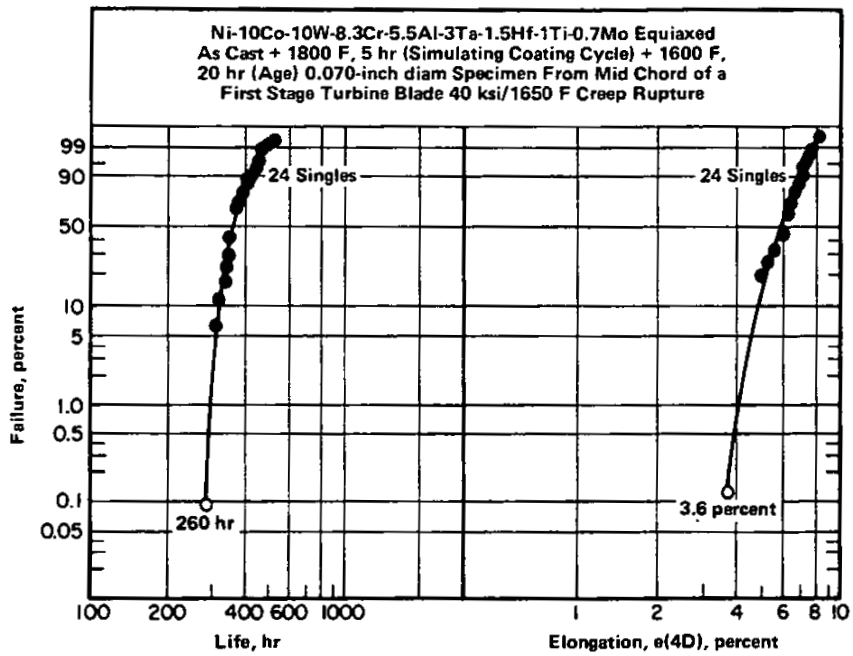

FIGURE 3.049. WEIBULL PROBABILITY PLOT OF CREEP-RUPTURE DATA FROM TESTS CONDUCTED AT 40 KSI AND 1650 F (8)

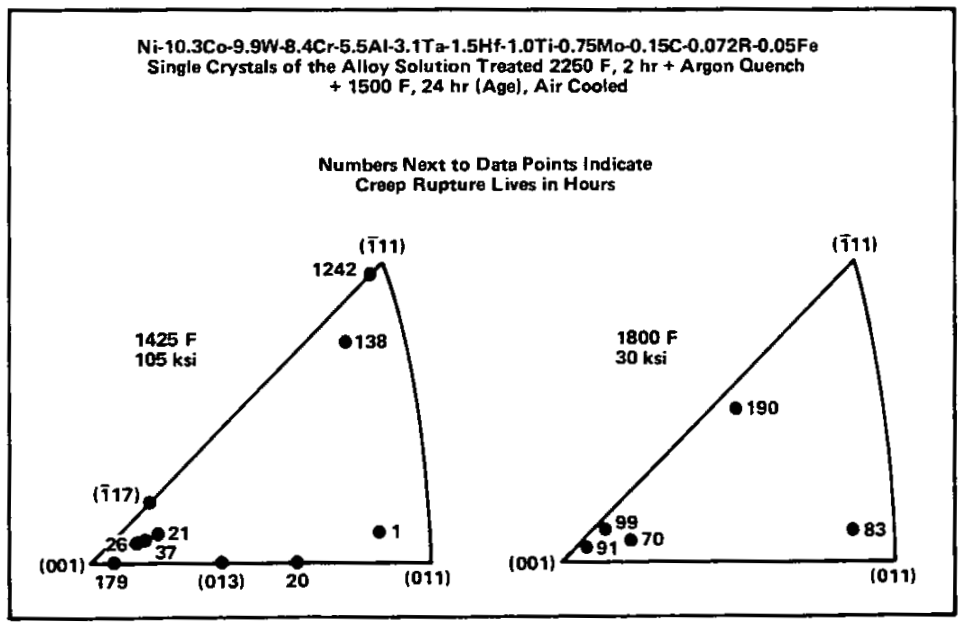

FIGURE 3.0410. EFFECT OF CRYSTALLOGRAPHIC ORIENTATION ON CREEP RUPTURE LIFE (4)

	Ni
10	Co
10	W
8.5	Cr
5.5	Al
0.7	Mo
3	Ta
1	Ti
1.4	Hf

MAR-M-247

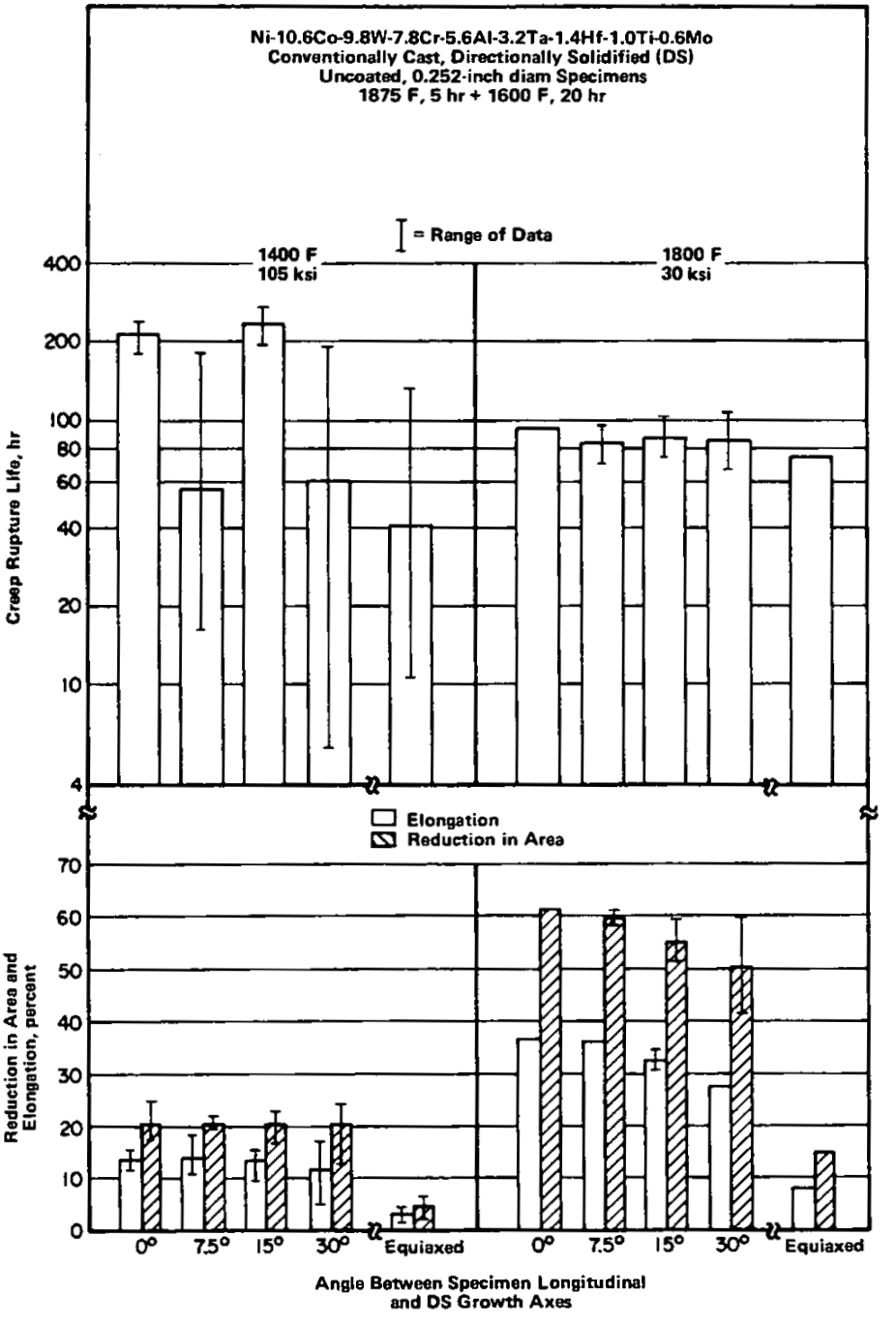

FIGURE 3.0411. EFFECT OF DS GRAIN ORIENTATION ON CREEP-RUPTURE PROPERTIES OF THE ALLOY AND COMPARISON WITH EQUIAXED ALLOY (3)

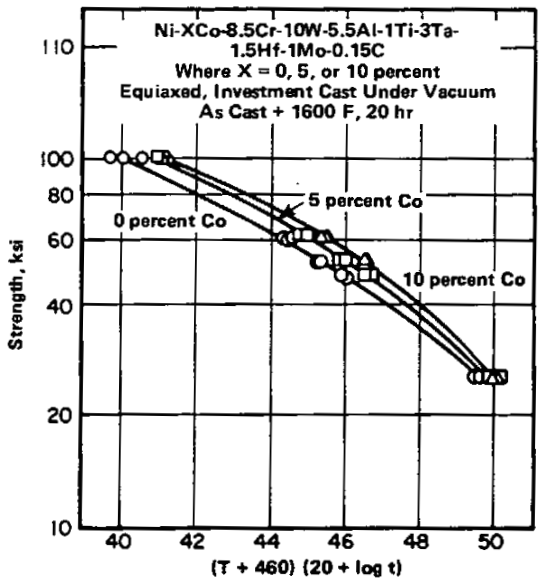

FIGURE 3.0412. LARSON-MILLER PLOT SHOWING EFFECT OF COBALT LEVEL ON CREEP-RUPTURE STRENGTH (9)

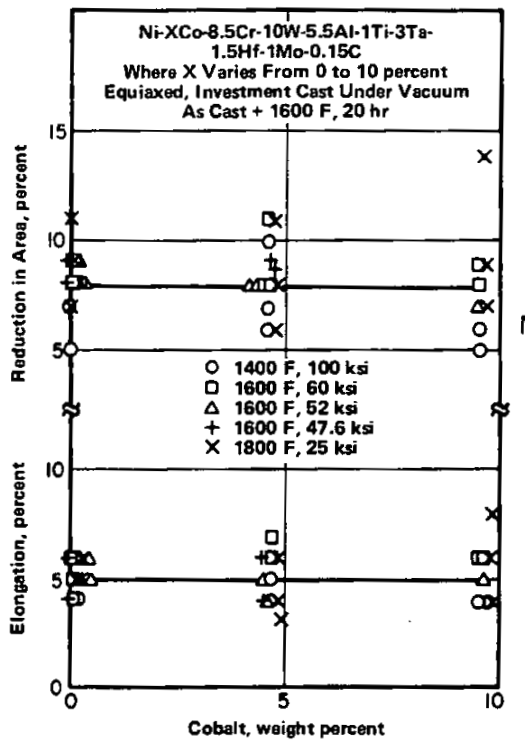

FIGURE 3.0413. EFFECT OF COBALT LEVEL IN THE ALLOY ON CREEP-RUPTURE DUCTILITY (9)

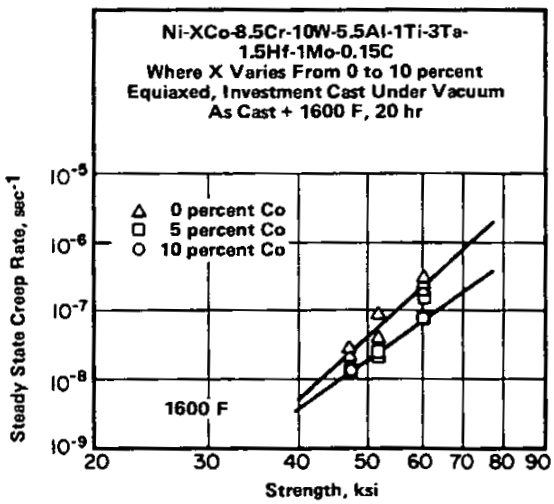

FIGURE 3.0414. EFFECT OF COBALT CONTENT ON CREEP RATE (9)

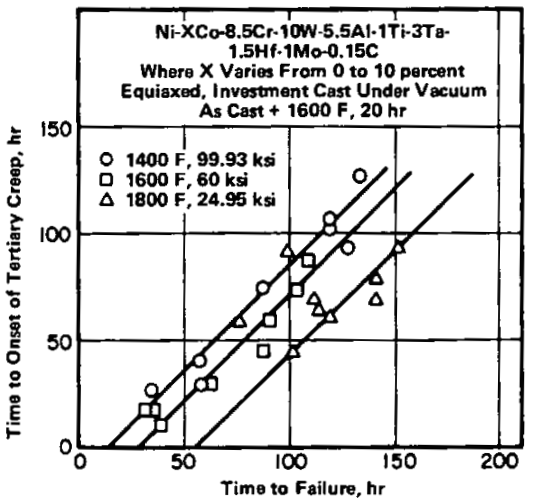

FIGURE 3.0415. EFFECT OF COBALT CONTENT ON TIME TO ONSET OF TERTIARY CREEP (9)

	Ni
10	Co
10	W
8.5	Cr
5.5	Al
0.7	Mo
3	Ta
1	Ti
1.4	Hf

MAR-M-247

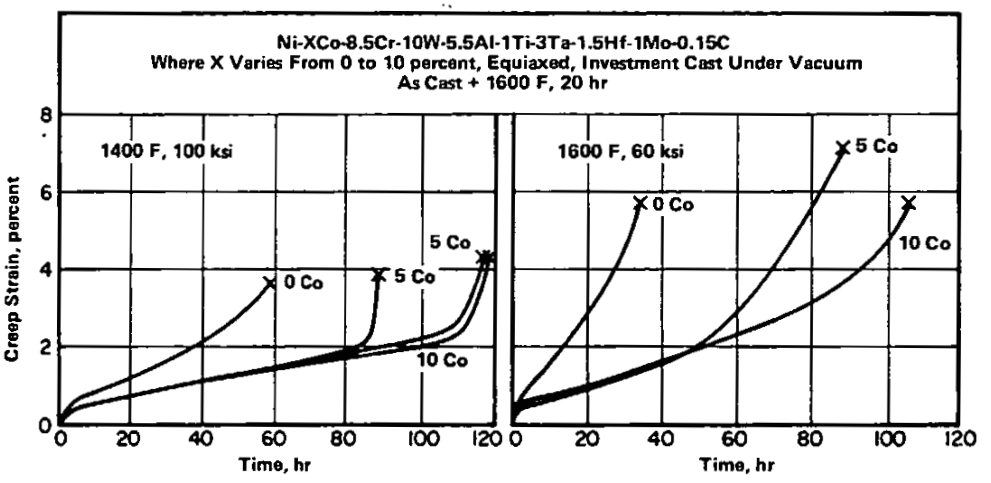

FIGURE 3.0416. EFFECT OF COBALT CONTENT ON CREEP CHARACTERISTICS OF THE ALLOY AT 1400 F, 100 KSI AND 1600 F, 60 KSI (9)

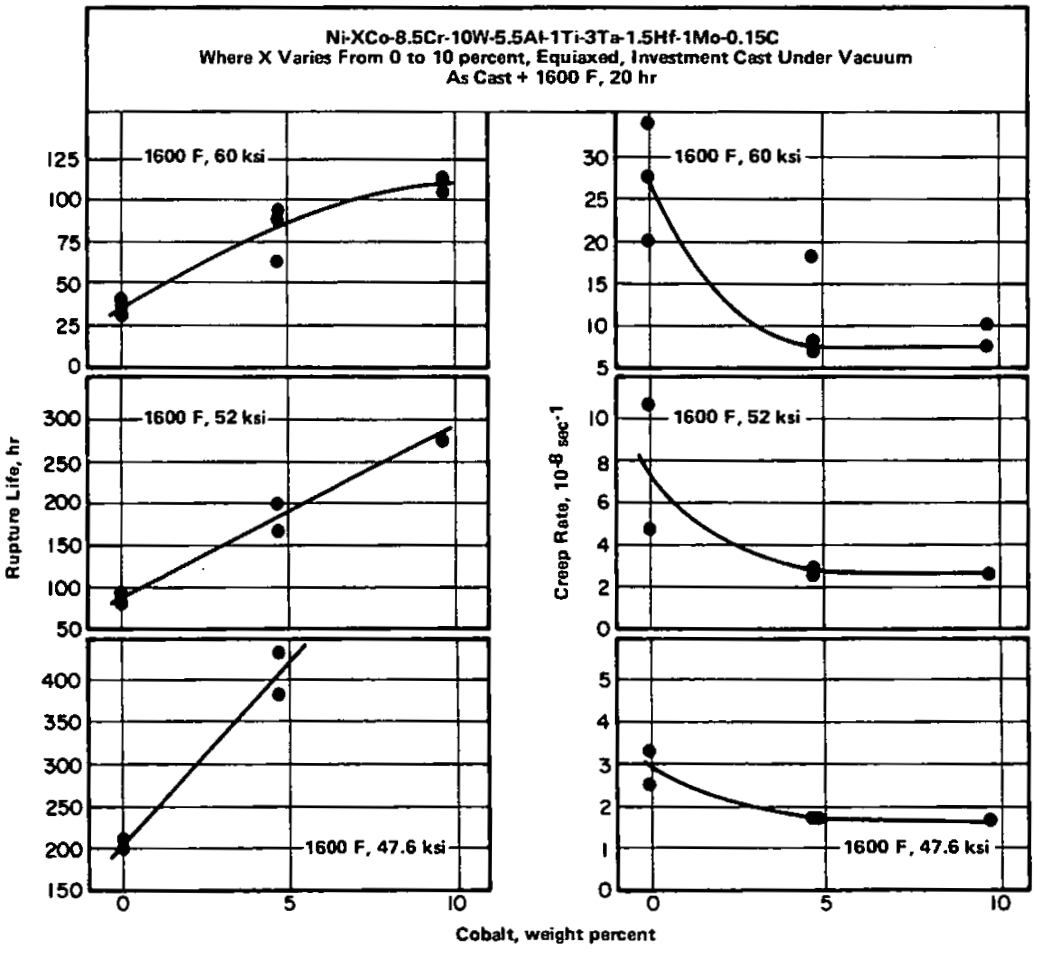

FIGURE 3.0417. EFFECT OF COBALT CONTENT ON CREEP RUPTURE AND STEADY STATE CREEP RATE AT 1600 F (9)

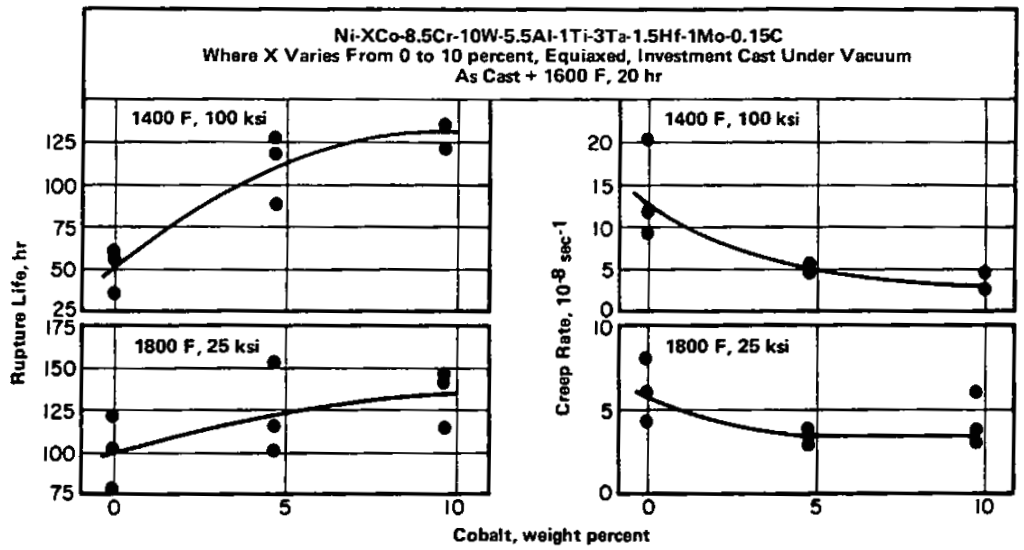

FIGURE 3.0418. EFFECT OF COBALT CONTENT ON CREEP RUPTURE AND STEADY STATE CREEP RATE AT 1400 F, 100 KSI AND 1800 F, 25 KSI (9)

Ni-10Co-8.4Cr-10W-5.5Al-1.05Ti-3.3Ta-1.4Hf-0.65Mo-0.15C-0.055Zr
For Actual Compsition of the Alloys, Refer to the Table Below
Modified Single Crystal Alloys Melted with Zirconia Crucibles
Heat Treatment Not Known

Alloy		MAR-M-247									
		Actual Alloy Composition, weight percent									
		Alloy 1		Alloy 2		Alloy 3		Alloy 4		Alloy 5	
Composition	Range	Master Melt	Blade	Master Melt	Blade	Master Melt	Blade	Master Melt	Blade	Master Melt	Blade
Mo	0.50-0.80	0.8	0.86	0.8	0.88	0.8	0.89	2.1	1.90	0.8	0.83
W	9.50-10.50	10.2	10.51	10.0	10.40	9.2	10.2	9.9	10.48	10.2	10.62
Ta	2.80-3.80	3.4	3.61	3.5	3.61	3.3	3.29	3.5	3.54	3.4	3.69
Ti	0.90-1.20	1.1	1.14	1.0	0.97	0.93	0.95	1.0	0.98	1.1	1.15
Cr	8.00-8.80	9.0	8.99	9.3	8.20	8.2	8.58	9.0	8.06	9.0	8.38
Co	9.00-11.00	0	–	–	–	5.1	5.45	–	–	–	–
Al	5.30-5.70	5.75	5.44	5.8	5.39	5.54	5.34	5.74	5.40	5.75	5.45
C	0.13-0.17	0.018	0.016	0.003	0.009	0.002	0.007	0.002	0.008	0.018	0.016
Hf	1.20-1.60	0	–	0.6	0.59	0.6	0.57	–	–	–	–
Zr	0.03-0.08	–	0.27	0.014	0.28	0.005	0.24	0.001	0.46	–	0.14
Y	–	0	–	–	–	–	–	–	–	0.4	0.04
Ni	Bal	Bal	Bal	Bal	Bal	Bal	Bal	Bal	Bal	Bal	Bal

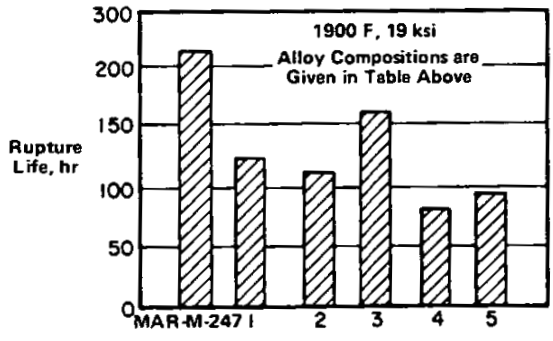

FIGURE 3.0419. EFFECT OF ZIRCONIUM CONTAMINATION ON CREEP-RUPTURE LIVES OF SPECIMENS MACHINED FROM SINGLE CRYSTAL BLADES IN LONGITUDINAL DIRECTION (7)

	Ni
10	Co
10	W
8.5	Cr
5.5	Al
0.7	Mo
3	Ta
1	Ti
1.4	Hf

MAR-M-247

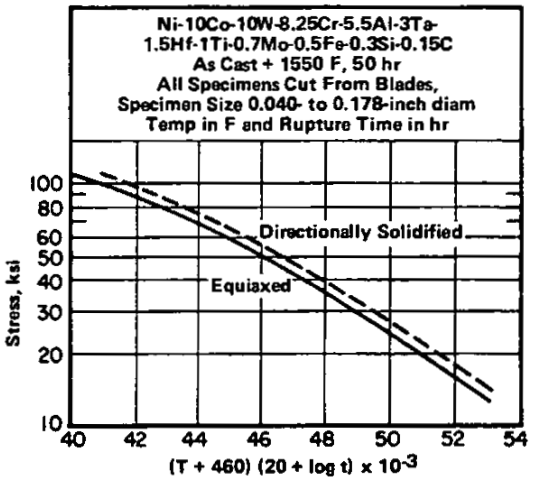

FIGURE 3.0420. LARSON-MILLER PARAMETERS FOR CREEP RUPTURE OF DIRECTIONALLY SOLIDIFIED AND EQUIAXED ALLOY (6)

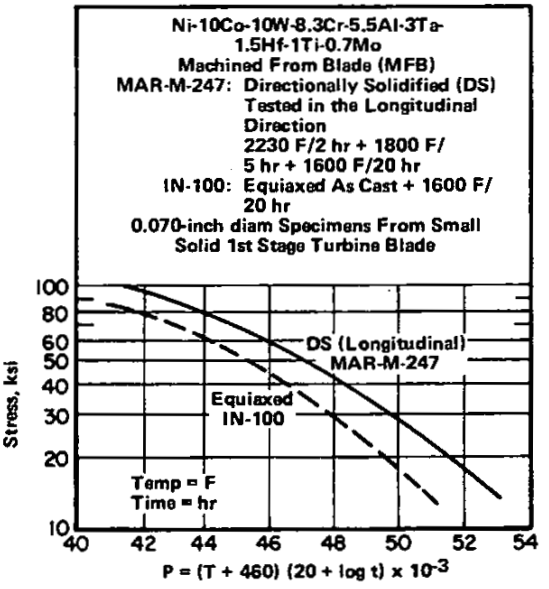

FIGURE 3.0421. LARSON-MILLER PARAMETERS FOR CREEP RUPTURE OF DIRECTIONALLY SOLIDIFIED MAR-M-247 AND EQUIAXED IN-100 (5)

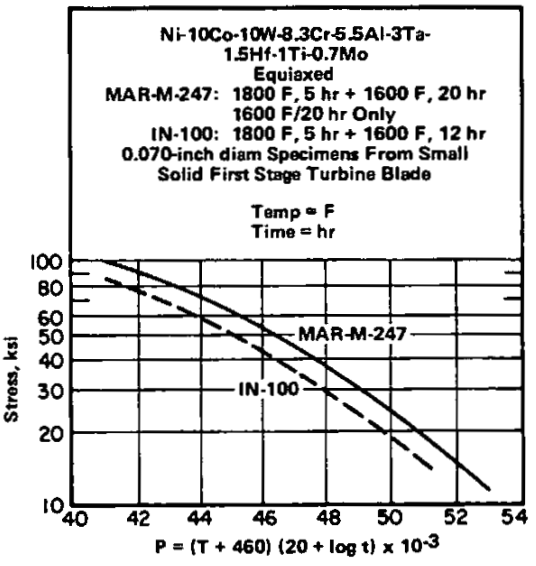

FIGURE 3.0422. COMPARISON OF LARSON-MILLER PARAMETERS FOR CREEP RUPTURE OF EQUIAXED MAR-M-247 AND IN-100 (5)

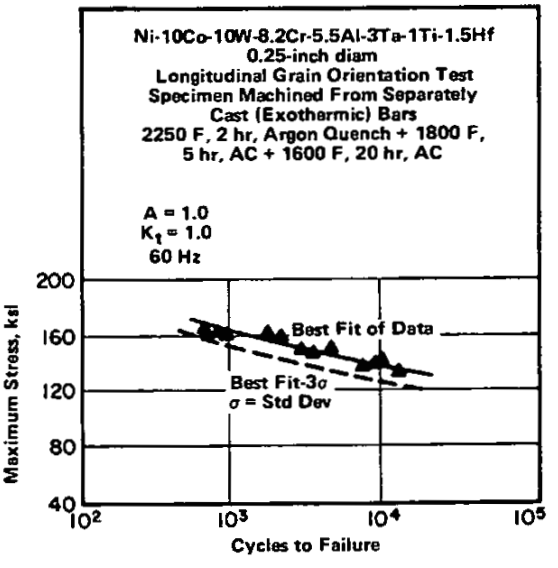

FIGURE 3.051. LOW CYCLE FATIGUE TESTS UNDER LOAD CONTROL AT 1400 F FOR SMOOTH UNCOATED SPECIMENS FROM SEPARATELY CAST TEST BARS (2)

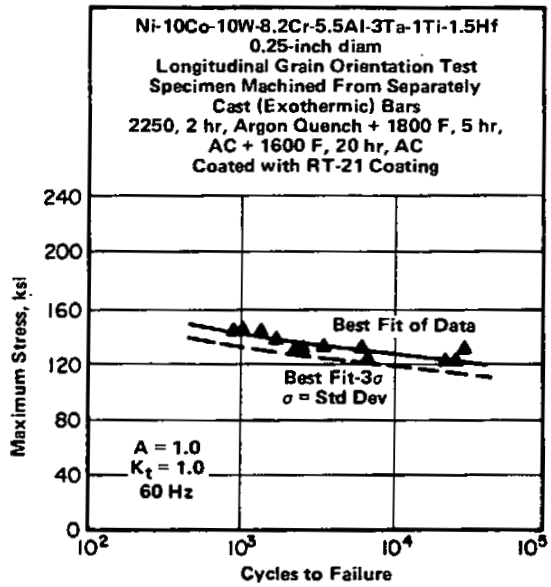

FIGURE 3.052. LOW CYCLE FATIGUE TEST UNDER LOAD CONTROL AT 1400 F FOR SMOOTH COATED SPECIMENS FROM SEPARATELY CAST TEST BARS (2)

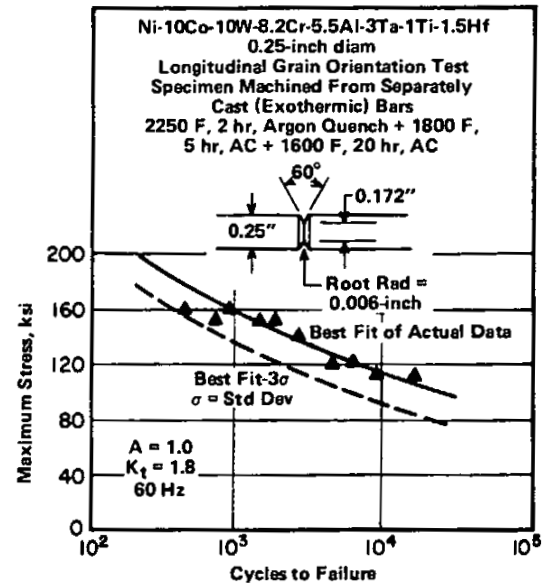

	Ni
10	Co
10	W
8.5	Cr
5.5	Al
0.7	Mo
3	Ta
1	Ti
1.4	Hf

MAR-M-247

FIGURE 3.053. LOW CYCLE FATIGUE TEST UNDER LOAD CONTROL AT 1400 F FOR NOTCHED UNCOATED SPECIMENS FROM SEPARATELY CAST TEST BARS (2)

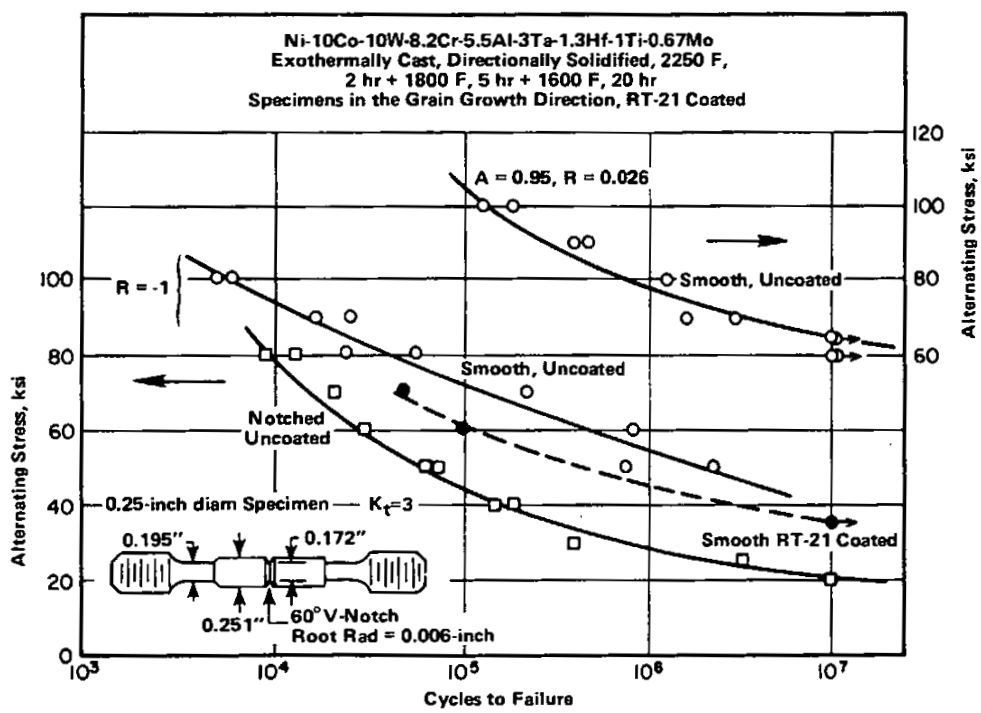

FIGURE 3.054. LOAD CONTROLLED HIGH CYCLE FATIGUE TESTS FOR SMOOTH AND NOTCHED SPECIMENS AT ROOM TEMPERATURE (2)

	Ni
10	Co
10	W
8.5	Cr
5.5	Al
0.7	Mo
3	Ta
1	Ti
1.4	Hf

MAR-M-247

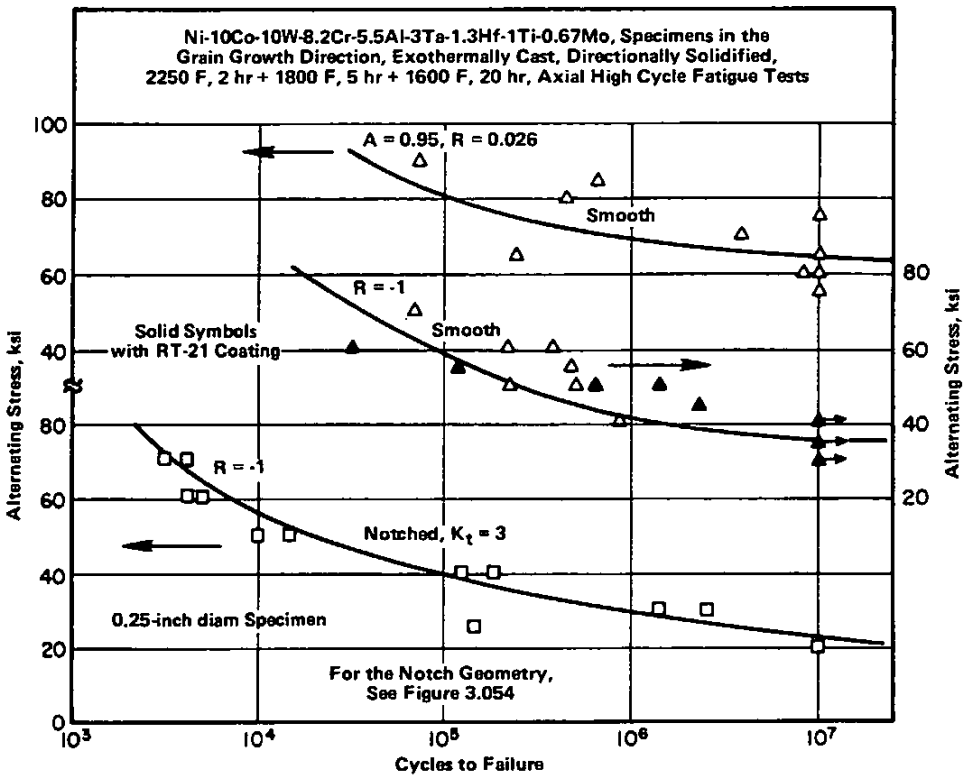

FIGURE 3.055. LOAD CONTROLLED HIGH CYCLE FATIGUE TESTS FOR SMOOTH AND NOTCHED SPECIMENS AT 1600 F (2)

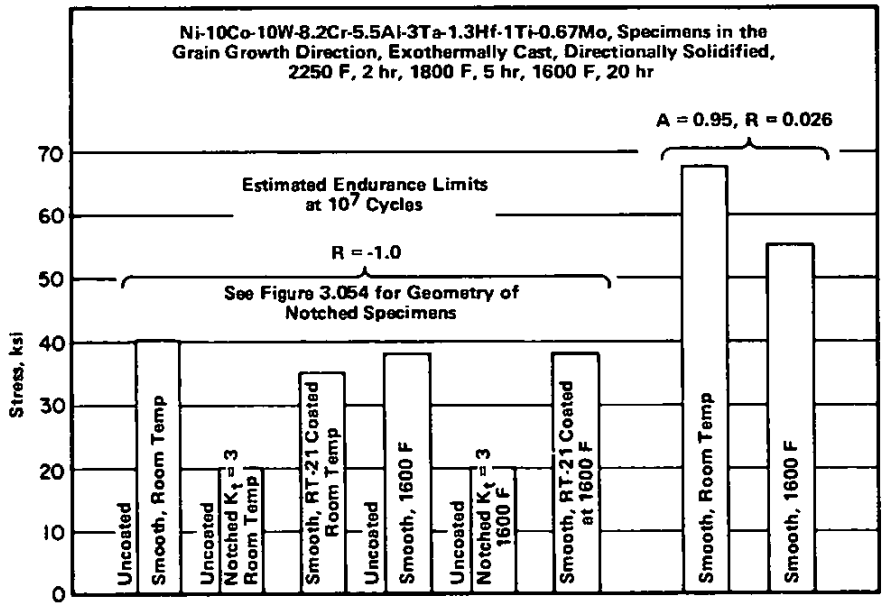

FIGURE 3.056. ESTIMATED ENDURANCE LIMITS AT 10^7 CYCLES FROM LOAD CONTROLLED AXIAL HIGH CYCLE FATIGUE TESTS (2)

	Ni
10	Co
10	W
8.5	Cr
5.5	Al
0.7	Mo
3	Ta
1	Ti
1.4	Hf

MAR-M-247

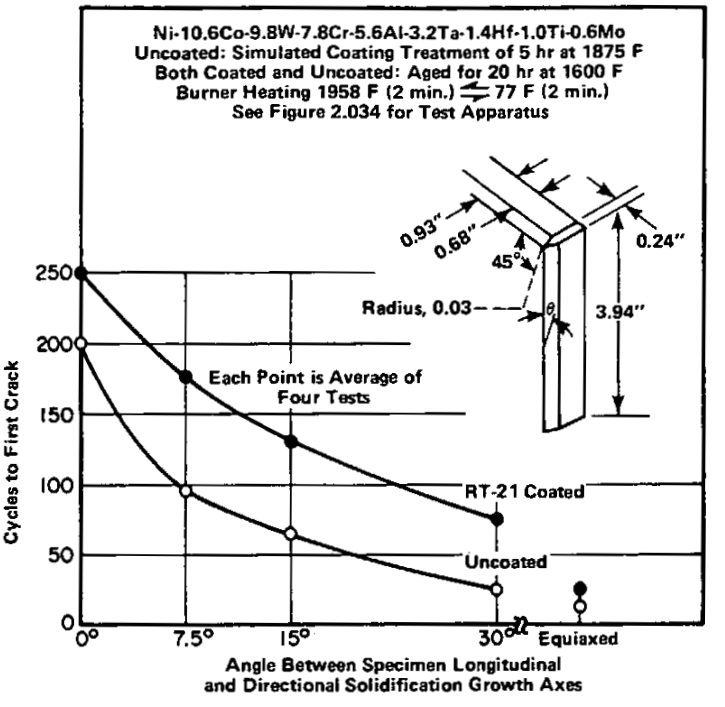

FIGURE 3.057. EFFECT OF GRAIN ORIENTATION ON THERMAL FATIGUE LIFE OF THE ALLOY IN THE COATED AND UNCOATED CONDITION (3)

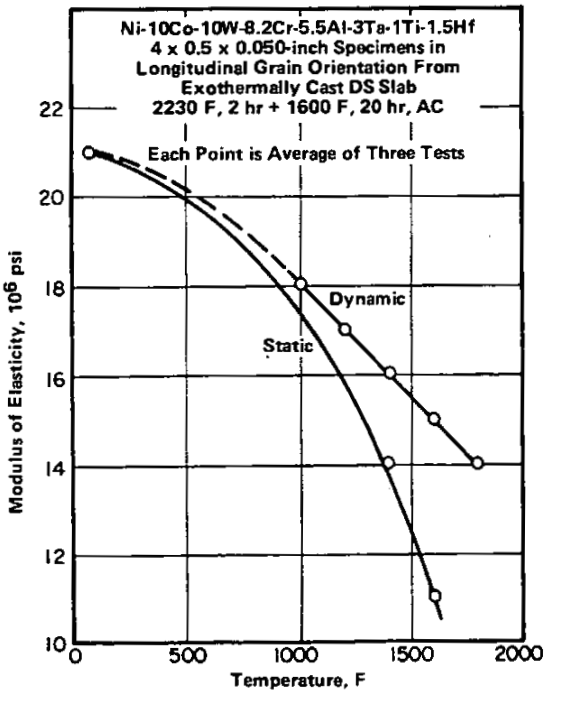

FIGURE 3.0621. MODULUS OF ELASTICITY IN LONGITUDINAL GRAIN ORIENTATION FOR TEST SPECIMENS MACHINED FROM EXOTHERMALLY CAST DIRECTIONALLY SOLIDIFIED ALLOY (2)